Available online at www.sciencedirect.com
SCIENCE DIRECT
Journal of Power Sources 155 (2006) 95–110
JOURNAL OF POWER SOURCES
www.elsevier.com/locate/jpowsour

Review

A review of anode catalysis in the direct methanol fuel cell

Hansan Liu [a], Chaojie Song [a], Lei Zhang [a], Jiujun Zhang [a,*], Haijiang Wang [a], David P. Wilkinson [a,b]

[a] *Institute for Fuel Cell Innovation, National Research Council Canada, Vancouver, BC, Canada V6T 1W5*
[b] *Department of Chemical and Biological Engineering, University of British Columbia, Vancouver, BC, Canada V6T 1Z4*

Received 10 November 2005; received in revised form 24 December 2005; accepted 5 January 2006
Available online 10 February 2006

Abstract

In this paper, more than 100 articles related to anode catalysts for the direct methanol fuel cell (DMFC) are reviewed, mainly focusing on the three most active areas: (1) progress in preparation methods of Pt–Ru catalysts with respect to activity improvement and utilization optimization; (2) preparation of novel carbon materials as catalyst supports to create a highly dispersed and stably supported catalysts; (3) exploration of new catalysts with a low noble metal content and non-noble metal elements through fast activity down-selection methods such as combinatorial methods. Suggested research and development (R&D) directions for new DMFC anode catalysis are also discussed.

Keywords: Direct methanol fuel cell; Anode catalyst; Pt–Ru alloy; Synthesis method; Carbon support; Combinatorial method

Contents

1. Introduction

Fuel cells, the energy converting devices with a high efficiency and low/zero emission, have been attracting more and more attention in recent decades due to high-energy demands, fossil fuel depletions, and environmental pollution throughout the world. For hydrogen gas fed fuel cells at their current technological stage, hydrogen production, storage, and transportation are the major challenges in addition to cost, reliability and durability issues. Direct methanol fuel cells (DMFCs), using liquid and renewable methanol fuel, have been considered to be a favourable option in terms of fuel usage and feed strategies [1,2]. Compared to hydrogen-fed fuel cells, which have a reforming unit, or low capacity in the hydrogen storage tank, DMFC uses a liquid methanol fuel, which is easily stored and transported and simplifies the fuel cell system.

* Corresponding author. Tel.: +1 604 221 3087; fax: +1 604 221 3001.
E-mail address: jiujun.zhang@nrc.gc.ca (J. Zhang).

0378-7753/$ – see front matter © 2006 Elsevier B.V. All rights reserved.
doi:10.1016/j.jpowsour.2006.01.030

It has been recognized that the success of fuel cell technology depends largely on two key materials: the membrane and the electro-catalyst. These two key materials are also directly linked to the major challenges faced in DMFCs, including (1) methanol crossover which can only be overcome by developing new membranes; (2) slow anode kinetics which can only be overcome by developing new anode catalysts. With regard to new DMFC anode catalysts, there are two major challenges, namely, the performance, including activity, reliability and durability, and cost reduction.

For DMFC anode catalyst performance improvement, the exploration of new catalyst materials including noble and non-noble metals is necessary. In this respect, an alloying strategy is one of the R&D directions. With the help of fast activity screening, a breakthrough could be accelerated to meet the requirements for DMFC commercialization. The other is a support strategy. Rapid development of nanotechnology, especially in the area of the synthesis of carbon nano-materials, will create more stable and active supported catalysts. Nanoparticle supported catalysts are believed to be the most promising materials for catalysis in PEM fuel cells including DMFCs.

Regarding cost reduction, for early DMFC commercialization, DMFC anode catalyst loadings must drop to a level of $<1.0\,mg\,cm^{-2}$ from the present 2.0–8.0 $mg\,cm^{-2}$, depending on applications. Loading reduction through increasing Pt utilization is one of the R&D directions. Alloying and nanoparticle supporting strategies could dramatically reduce the Pt content in the catalysts without performance compromise. Non-noble catalyst development is the other approach for catalyst cost reduction. However, at this current stage, non-noble DMFC anode catalysts are not yet feasible. A more thorough exploration is needed in this area. Real breakthroughs in DMFC anode catalysis are necessary with respect to performance and cost. In order to make fuel cell technology, including DMFC technology a success, new catalyst exploration for performance improvement and cost reduction remains the major challenge.

Great progress has been achieved during the last decade in fuel cell science and technology, especially in some application areas such as portable, transportation, and stationary power sources [3]. However, the commercialization of DMFCs is still hindered by some technical challenges. As mentioned above, two major ones are sluggish methanol oxidation kinetics even on some state-of-the-art anode catalysts, and methanol crossover through the membrane, which not only depresses cathode performance, but also reduces fuel efficiency. Currently, most research has focused on these two areas, exploring new anode catalysts that can effectively enhance the methanol electro-oxidation kinetics, and seeking new membranes that have a low methanol crossover. In an effort to reduce cathode performance depression induced by methanol crossover, some activities on methanol-tolerant cathode catalysts have also been carried out [4].

It seems that there are limited electrode materials that are suitable for use in methanol oxidation electro-catalysis, especially with an acidic DMFC electrode/membrane interface. Only platinum/ruthenium alloys, which show reasonable activities and stability, are the most practical electro-catalysts for the DMFC application. For a pure platinum catalyst, the adsorption of CO, one of the intermediates in methanol electro-oxidation, can occupy the reaction active sites, resulting in slow reaction kinetics. When a second metal, such as ruthenium, alloys with platinum the oxidation kinetics of methanol are improved significantly reaching a practicable level. The mechanism of methanol oxidation on the Pt surface has been investigated extensively for decades. According to a well-described mechanism [5], the primary processes of methanol oxidation on the Pt surface include several steps such as: (1) methanol adsorption; (2) C–H bond activation (methanol dissociation); (3) water adsorption; (4) water activation; (5) CO oxidation. The formation of OH by water activation on the Pt surface, which is a necessary step for the oxidative removal of adsorbed CO, requires a high potential. In terms of methanol anode oxidation, such a high potential will limit the fuel cell application of a pure platinum catalyst. As mentioned above, a second metal that can provide oxygenated species at lower potentials for oxidative removal of adsorbed CO is definitely needed. Binary Pt-based alloys, such as PtRu, PtOs, PtSn, PtW, PtMo, etc., have been investigated in order to improve the electro-oxidation activities of methanol. Among them, the Pt–Ru alloy has been found to be the most active binary catalyst and is the state-of-the-art anode catalyst for DMFCs. The enhanced activity of the Pt–Ru catalyst when compared with Pt for methanol oxidation has been attributed to both a bi-functional mechanism [6] and a ligand (electronic) effect [7]. The bi-functional mechanism involves the adsorption of oxygen containing species on Ru atoms at lower potentials thereby promoting the oxidation of CO to CO_2, which can be summarized as follows [6]:

$$Pt + CH_3OH \rightarrow PtCO_{ads} + 4H^+ + 4e^- \quad (1)$$

$$Ru + H_2O \rightarrow Ru(OH)_{ads} + H^+ + e^- \quad (2)$$

$$PtCO_{ads} + Ru(OH)_{ads} \rightarrow CO_2 + Pt + Ru + H^+ + e^- \quad (3)$$

The catalytic activity of the Pt–Ru catalyst is strongly dependent on the composition, structure, morphology, particle size and alloyed degree.

As reviewed by Arico et al. [2] and Lamy et al. [5], many works have been devoted to the performance optimization of Pt–Ru catalysts towards methanol oxidation. The current consensus is that the optimal Pt/Ru ratio is 1:1, and the particle sizes are better brought down to the nanoscale in order to improve catalyst utilization. However, from the practical standpoint in a real fuel cell environment, a high catalyst loading ($\sim$2–8 $mg\,cm^{-2}$) is required, even when using a 1:1 Pt–Ru alloy catalyst, in order to achieve acceptable fuel cell performance, especially when considering the lifetime of the fuel cell. This high noble catalyst loading will definitely cause costs to be high, hindering the commercialization of DMFCs. Therefore, the reduction of the catalyst loading through further improvement of activity and optimization of catalyst utilization is necessary. Exploring new catalysts such as non-noble catalysts [8] and catalyst activity optimization through supporting tactics such as nano-material supporting strategy [9] are two important approaches.

In this paper, the development of DMFC anode catalysts in recent years is reviewed, mainly focusing on the three most

active areas, i.e., catalyst preparation method development, carbon supporting strategies, and a combinatorial method for new catalyst screening.

2. Catalyst preparation methods

In recent years, methodological development for Pt–Ru catalyst preparation has been one of the major topics in DMFC anode catalyst exploration. The Pt–Ru catalyst has been supported on some high-surface-area materials, such as carbon particles, in order to achieve high dispersion and maximum utilization, as well as to avoid catalyst agglomeration during the fuel cell operation. Although unsupported Pt–Ru catalysts have also drawn some attention in recent years [10–12], the latest reports have focused primarily on supported Pt–Ru/C catalysts. The common criteria for a high performance catalyst are: (1) a narrow nanoscale size distribution; (2) a uniform composition throughout the nanoparticles; (3) a fully alloyed degree; (4) high dispersion on carbon support. According to these criteria, some innovative and cost-effective preparation methods have been developed and show promise for reaching performance optimization by controlling synthetic procedures and conditions. There are three important methods for preparing carbon-supported Pt–Ru catalysts, including the impregnation method, the colloidal method and the microemulsion method. All of these include a chemical step for forming nanoparticles, and a deposit step for dispersing the catalyst onto the carbon particles, as summarized schematically in Fig. 1.

2.1. The impregnation method

Of those three methods, the impregnation method is the most widely used, and is a simple and straightforward chemical preparation technique for Pt–Ru catalyst preparation [13–36]. The impregnation method includes an impregnation step, followed by a reduction step. During the impregnation step, Pt and Ru precursors are mixed with high-surface-area carbon black in aqueous solution to form a homogeneous mixture. As a catalyst support, carbon black plays a major role in terms of penetrating and wetting the precursors, and it can also limit nanoparticle growth. The chemical reduction step can be carried out by liquid phase reduction using $Na_2S_2O_3$, $NaBH_4$, $Na_4S_2O_5$, N_2H_4 or formic acid as a reductive agent, or gas phase reduction using a flowing hydrogen stream as a reductive agent under elevated temperature.

During the impregnation process, many factors can affect the composition, morphology and dispersion of Pt–Ru/C catalyst, resulting in the variation of catalytic activity. The porosity of carbon black support can effectively control the catalyst nanoparticle size and dispersion, which will be discussed in the next section. Many studies have indicated that synthetic conditions, such as the nature of the metal precursors used, the reduction method and the heating temperature, are also crucial in the impregnation process [13,17–20]. Generally, metal chloride salts (e.g., H_2PtCl_6 and $RuCl_3$) are commonly used as precursors in the impregnation–reduction process due to their easy availability. However, it was argued that the metal chloride salts might lead to chloride poisoning, reducing the dispersion

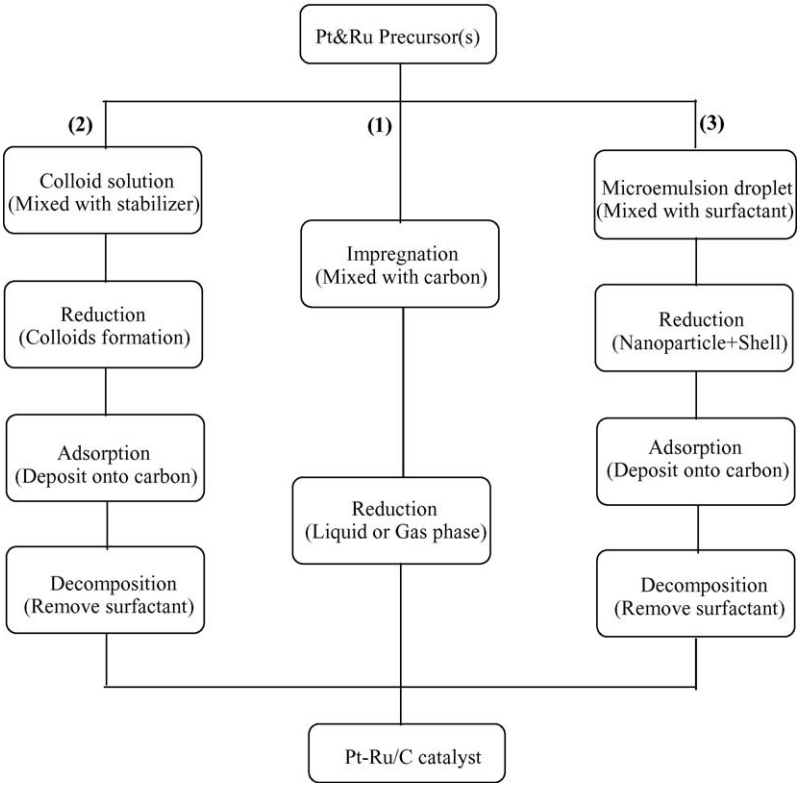

Fig. 1. Synthesis methods for Pt–Ru/C catalysts: (1) The impregnation method, (2) the colloidal method and (3) the microemulsion method.

degree, catalytic activity and stability of the Pt–Ru/C catalyst. In order to reduce the poisoning of chloride, some work has been devoted to the approach of a chloride-free impregnation method. An alternative process has been suggested using metal sulphite salts (e.g., $Na_6Pt(SO_3)_4$, $Na_6Ru(SO_3)_4$) as precursors, which can be prepared from the chloride metal salts [20–22]. Other Cl-free compounds such as $Pt(NH_3)_2(NO_2)_2$, $RuNO(NO_3)_x$, $Pt(NH_3)_4(OH)_2$, $Pt(C_8H_{12})(CH_3)_2$, and $Ru_3(CO)_{12}$ were also used as metal precursors in the impregnation method [13,18,27]. These Cl-free routes were validated and could give Pt–Ru/C catalysts higher dispersion states and better catalytic activity compared with the conventional Cl-containing route. For example, Takasu et al. [13] reported that Pt–Ru/C catalysts synthesized using different salts such as chloride, nitrate, and carbonyl showed mass-specific current density of 8, 32 and 57 mA $mg^{-1}_{(PtRu)}$, respectively, measured at 500 mV (versus RHE) in 1.0 M H_2SO_4 + 0.5 M CH_3OH at 60 °C.

Recently, Dickinson et al. [20] prepared some Pt–Ru/C catalysts by direct thermal decomposition of Pt and Ru carbonyl complexes (i.e., $[Pt(CO)_2]_x$ and $[Ru_3(CO)_{12}]$) onto carbon support. Their results showed that the catalytic activity is favourably comparable with those commercially available and with sulphito-route prepared Pt–Ru/C catalysts. The catalyst prepared by carbonyl-route showed a mass specific activity of 340 A $g^{-1}_{(PtRu)}$ at 0.2 V (versus MMS) during a polarization testing in 1.0 M H_2SO_4 + 1.5 M CH_3OH at 65 °C. If using sulphito-route, the activity was 260 A $g^{-1}_{(PtRu)}$. Both of activities are comparable to that of commercially available catalyst (E-TEK with a value of 220 A $g^{-1}_{(PtRu)}$). The reference electrode was Hg/Hg_2SO_4. Two advantages of this route over other procedures are obvious: one is the easy preparation of Pt and Ru carbonyl complexes by direct oxidation of a metal chloride salt with carbon monoxide, and the other is the simplification of the steps by eliminating the reduction step. A drawback of this route is that Ru carbonyl decomposition is more favourable than Pt carbonyl decomposition, resulting in a Ru-rich product. In order to improve that, another modified impregnation route using single-source metal precursors was recently developed [28–34], where single-source precursors were used for the thermal decomposition process to produce Pt–Ru nanoparticles on carbon black support under a reductive H_2 atmosphere. These single-source precursors include molecular clusters, such as $PtRu_5C(CO)_{16}$, $Pt_2Ru_4(CO)_{16}$ [28,29], and organometallic complexes, such as $(\eta\text{-}C_2H_4)(Cl)Pt(\mu\text{-}Cl)_2Ru(Cl)(\eta^3$: η^3-2,7-dimethyloctadienediyl), $(Ph_3P)(Cl)Pt(\eta\text{-}Cl)_2Ru(Cl)$ (η^3: η^3-2,7-dimethyloctadienediyl), $(Et_3P)(Cl)Pt(\eta\text{-}Cl)_2Ru(Cl)(\eta^3$: η^3-2,7-dimethyloctadienediyl) ($[(2,2'$-bipyridine$)_2Ru(\mu$-2,2′-bipyrimidine$)PtCl_2][BF_4]_2$, $[(2,2'$-bipyridine$)_2Ru(\mu$-2,2′-bipyrimidine$)PtCl_2][PF_6]_2$ [30–32], and $[(bipy)_3Ru](PtCl_6)$ [33]. To reduce the effect of thermal treatment on particle size, microwave dielectric loss heating was also introduced into this route [34]. Because the metal composition is pre-controlled, this route is advantageous for preparing stoichiometric and homogeneous Pt–Ru catalysts with a narrow size distribution. However, the synthesis of these single-source precursors is too complicated and uses too many organic compounds, which may limit its application. Table 1 lists various Pt–Ru/C catalysts prepared by different routes of the impregnation method together with physical characterization and electrochemical measurement.

The major drawback of the impregnation method is the difficulty in controlling nanoparticle size and distribution. However, a highly dispersed Pt–Ru/C catalyst can still be obtained by carefully controlling appropriate preparation conditions. Yang et al. [35] recently prepared a highly dispersed Pt–Ru/C catalyst with metal loading as high as 60 wt.% and a narrow size distribution (1.5 ± 0.5 nm, as shown in Fig. 2) even using chlorine-containing precursors. More recently, Guo et al. [36] reported a modified impregnation method using citric acid as stabilizer of metal ions to prepare well-dispersed Pt–Ru/C catalysts. Their in-house Pt–Ru/C catalyst gave a power density of 44 mW cm^{-2} in a single DMFC testing at 70 °C, which was comparable to the power density of 42 mW cm^{-2} for a commercially available E-TEK catalyst with the same composition at the similar testing conditions.

Table 1
Summary of the reported Pt–Ru/C catalysts synthesized by different preparation routes of the impregnation method

Catalyst	Precursor/reducing agent	Particle size (nm)	Activity	Measurement protocol	Reference
20t% $Pt_{75}Ru_{25}$	H_2PtCl_6, $RuCl_3$/HCOOH	2–5	300 mA cm^{-2} at 400 mV, 1 mg cm^{-2}	A single DMFC, 2 M CH_3OH, O_2, 70 °C	[15]
20% $Pt_{50}Ru_{50}$	H_2PtCl_6, $RuCl_3$/$NaBH_4$	3.7 ± 1.0	4 mA cm^{-2} at 200 mV (vs. SCE)	CV (vitreous carbon) 1 M H_2SO_4 + 2 M CH_3OH, RT	[33]
30% $Pt_{67}Ru_{33}$	H_2PtCl_6, $RuCl_3$/H_2	1.5 ± 0.5	65 mA mg^{-1} at 400 mV (vs. RHE), 0.25 mg cm^{-2}	Polarization (glassy carbon) 0.5 M H_2SO_4 + 2 M CH_3OH, 60 °C	[35]
50% $Pt_{50}Ru_{50}$	$Na_6Pt(SO_3)_4$, $Na_6Ru(SO_3)_4$/H_2	~2	60 mA mg^{-1} at 400 mV (vs. RHE), 2 mg cm^{-2}	Polarization (carbon paper) 1 M H_2SO_4 + 1.5 M CH_3OH, 65 °C	[22]
30% $Pt_{50}Ru_{50}$	$Pt(NH_3)_2(NO_2)_2$, $RuNO(NO_3)_x/H_2 + N_2$	3.1 ± 0.5	8 mA mg^{-1} at 400 mV (vs. RHE), 0.06 mg cm^{-2}	Polarization (glassy carbon), 0.5 M H_2SO_4 + 1 M CH_3OH, 60 °C	[13]
50% $Pt_{50}Ru_{50}$	$[Pt(CO)_2]_x$, $Ru_3(CO)_{12}$/none	2.5 ± 0.45	85 mA mg^{-1} at −200 mV (vs. MMS), 1 mg cm^{-2}	Polarization (carbon paper) 1 M H_2SO_4 + 1.5 M CH_3OH, 65 °C	[20]
30% $Pt_{50}Ru_{50}$	$(\eta\text{-}C_2H_4)(Cl)Pt(\mu\text{-}Cl)_2Ru(Cl)(\eta^3$: η-2,7-dimethyloctadienediyl)/H_2	3.5–5.4	120 mA cm^{-2} at 400 mV, 2.43 mg cm^{-2}	A single DMFC, 1 M CH_3OH, air, 90 °C	[30]

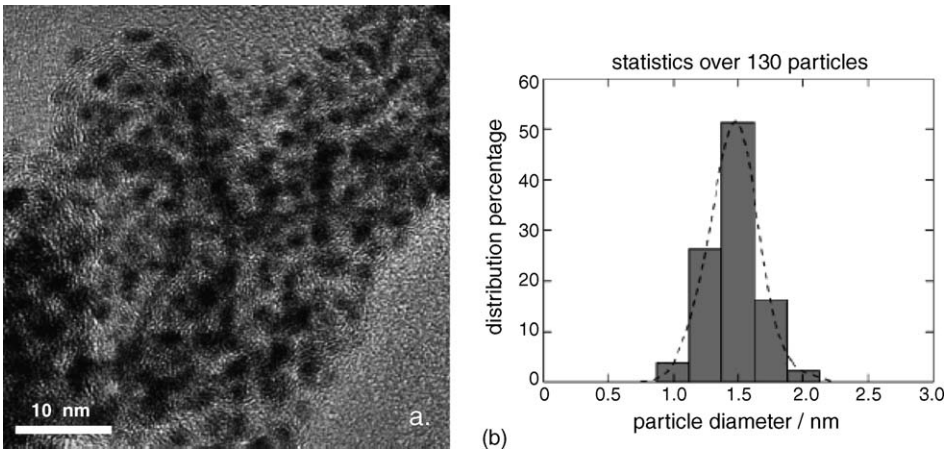

Fig. 2. (a) HRTEM image and (b) statistics histogram of the particle size distribution for Pt–Ru/C electrocatalyst (40 wt.% Pt + 20 wt.% Ru) prepared by the impregnation method [35].

2.2. The colloidal method

The colloidal method is another extensively explored preparation route for the Pt–Ru/C catalyst [37–53]. Usually, the colloidal method includes the following common steps: (1) preparation of Pt–Ru containing colloids; (2) deposition of the colloids onto the carbon support; (3) chemical reduction of the mixture. There are several colloidal routes with distinguishable preparation conditions in the steps, as listed in Table 2.

Watanabe et al. [37] reported a preparation procedure for a highly dispersed Pt–Ru catalyst through co-deposition of colloidal Pt and Ru oxides on carbon in aqueous media, followed by a reduction with bubbling hydrogen. A modified Watanabe's route using metal sulphite slats, with a final thermal treatment in an H_2 atmosphere was successful in producing a catalyst with a better performance [38,39]. This metal oxide colloids route can prepare a Pt–Ru catalyst with much higher specific surface area compared with that of a conventional impregnation method. However, the particle growth and agglomeration control in this route seem to be problematic.

Bönnemann et al. [40–44] developed an organometallic colloid route by stabilizing the Pt/Ru metal particles with organic molecules, resulting in easy control of particle size and distribution. Bönnemann's route mainly consists of three steps, i.e. pre-forming surfactant-stabilized Pt–Ru colloids (e.g., PtRu-$N(oct)_4Cl$ colloids), adsorbing the colloids on high-surface-area carbon, and removing the organic stabilizer shell by thermal treatment in an O_2 atmosphere and H_2 atmosphere, respectively. By this route, Pt–Ru catalysts with well-defined, completely alloyed particles and a very narrow particle size distribution (<3 nm) were obtained, and showed comparable activity ($\sim 70\,mA\,mg^{-1}_{(PtRu)}$ at 500 mV (versus RHE) in 0.5 M CH_3OH + 0.5 M H_2SO_4 at 60 °C) with that of state-of-the-art commercially available catalyst ($\sim 80\,mA\,mg^{-1}_{(PtRu)}$ at the

Table 2
Summary of the reported Pt–Ru/C catalysts synthesized by different preparation routes of the colloidal method

Catalyst	Precursor	Reducing agent/stabilizer	Particle size (nm)	Activity	Measurement protocol	Reference
30% $Pt_{50}Ru_{50}$	H_2PtCl_6, $RuCl_3$	$H_2O_2 + H_2$/none	3–4	200 mA cm^{-2} at 400 mV (vs. RHE), 2 mg cm^{-2}	Polarization (gas diffusion electrode) 1.5 M H_2SO_4 + 2 M CH_3OH (vapor), 60 °C	[37]
20% $Pt_{50}Ru_{50}$	$PtCl_2$, $RuCl_3$	$NOct_4[BEt_3H]$/itself	1.5 ± 0.4	20 mA mg^{-1} at 400 mV (vs. RHE), 0.014 mg cm^{-2}	Potentiostatic (glassy carbon) 0.5 M H_2SO_4 + 2 M CH_3OH, 60 °C	[44]
20% $Pt_{50}Ru_{50}$	$Pt(acac)_2$, $Ru(acac)_3$	$Al(CH_3)_3$/itself	1.5 ± 0.5	27 mA mg^{-1} at 400 mV (vs. RHE), 0.014 mg cm^{-2}	Potentiostatic (glassy carbon) 0.5 M H_2SO_4 + 2 M CH_3OH, 60 °C	[45]
30% $Pt_{50}Ru_{50}$	$Pt(dba)_2$, $Ru(COD)(COT)$	$(C_8H_{17})_4NDCTA$/itself	<2	18 mA mg^{-1} at 400 mV (vs. RHE), 0.007 mg cm^{-2}	Potentiostatic (glassy carbon) 0.5 M H_2SO_4 + 0.5 M CH_3OH, 60 °C	[46]
27% $Pt_{67}Ru_{33}$	H_2PtCl_6, $RuCl_3$	1-Propanol/PVP	2–3.2	220 mA mg^{-1} at 400 mV, 0.27 mg cm^{-2}	A single DMFC, 1.5 M CH_3OH, O_2, 80 °C	[49]
20% $Pt_{50}Ru_{50}$	H_2PtCl_6, $RuCl_3$	Ethylene glycol/itself	3–6	1.1 mA at 400 mV (vs. SCE), 46% decay after 1 h	Chronoamperometry (vitreous carbon) 1 M H_2SO_4 + 2 M CH_3OH, RT	[51]
30% $Pt_{67}Ru_{33}$	H_2PtCl_6, $RuCl_3$	Ethylene glycol/itself	2.0 ± 0.3	300 mA cm^{-2} at 400 mV, 2 mg cm^{-2}	A single DMFC, 1.0 M CH_3OH, O_2, 90 °C	[52]

similar testing conditions) [44]. To simplify the preparation steps and avoid using chloride-containing stabilizers, Paulus et al. [45] developed a modified route by using organoaluminium molecules (e.g., $Al(CH_3)_3$) as both the reductive agent and stabilizer. The prepared Pt–Ru–Al/C catalyst with narrow size distribution (1.3 ± 0.4 nm) showed good size-stabilization even under thermal treatment, and at the same time, the durability was also improved. However, a slightly lower activity (less than that of $PtRu(NR_4)$/C catalyst by 25–50%) towards methanol oxidation was observed due to residual aluminium oxide on the catalyst surface [45]. Recently, another chloride-free route, using the so-called "Armand's Ligand" as a stabilizer, was reported by Bönnemann et al. [46]. Their results indicated that highly dispersed Pt–Ru catalysts prepared by this route had excellent methanol oxidation activities ($\sim 62\,mA\,mg^{-1}_{(metal)}$ at 500 mV (versus NHE) in 0.5 M CH_3OH + 0.5 M H_2SO_4 at 60 °C) compared with commercially available catalysts (E-TEK) ($\sim 50\,mA\,mg^{-1}_{(metal)}$ at the same conditions). This can be attributed to both the smaller particle sizes (<2 nm) and the impurity-free surfaces. Organometallic stabilization was also integrated into the metal oxide colloid route to prepare some surfactant-stabilized PtRuOx fine colloids with a narrow size distribution of 1.5 ± 0.4 nm [47]. As a tuneable synthesis method, Bönnemann's route is favourable for controlling the composition, size and shape of the catalyst or other multi-metallic alloy nanoparticle. There are several advantages and some promising results shown by Bönnemann's route. The organometallic colloid route is still not favourable in practical applications due to the complexity of the preparation steps and the relatively high cost.

Other colloid routes using various reducing agents, organic stabilizers or shell-removing approaches have also been developed in recent years. Wang and Hsing [48] and Kim et al. [49] prepared Pt–Ru catalysts based on an alcohol reduction method using dodecyldimethyl(3-sulfo-propyl) ammonium hydroxide (SB12) and polyvinylpyrrolidone (PVP) as a stabilizer, respectively. Bensebaa et al. [50] reported the preparation of Pt–Ru nanoparticles using ethylene glycol as both a solvent and reducing agent, and PVP as a stabilizer. Liu et al. [51] developed a glycol colloid route in which an organic stabilizer was unnecessary. Pt–Ru colloids were prepared in an ethylene glycol solution and subsequently transferred to a toluene medium with decanethiol as the phase transfer agent. The microwave method was used to remove the organic shell from these colloids [50,51]. More recently, Xue et al. [52] reported a two-step spray pyrolysis route to synthesize highly dispersed Pt–Ru/C catalysts, in which Pt and Ru precursors were mixed with poly(ethylene glycol) and Vulcan XC-72R to form an aerosol by an atomizer. Then the aerosol droplets were forced to pass through a heated quartz tube in which Pt–Ru nanoparticles formed on the carbon support by solvent evaporation and precursor decomposition. The prepared 30 wt.% Pt–Ru/C catalyst showed a cell voltage of 0.39 V, comparable to 0.34 V for the commercially available catalyst (E-TEK) at a current density of 300 mA cm^{-2} in a DMFC testing at 90 °C (Fig. 3). The tuneable colloid method is simple and very promising in Pt–Ru/C catalyst preparation.

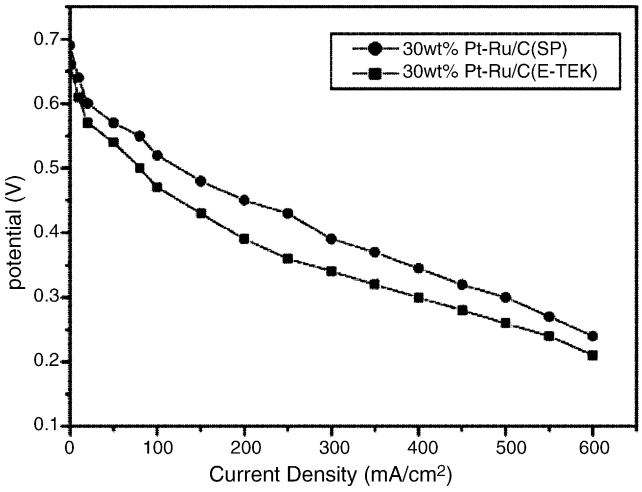

Fig. 3. DMFC performance comparison between two Pt–Ru/C catalysts. One was prepared by a spray pyrolysis (SP) method and the other is commercially available (E-TEK). Cathode: 30 wt.% Pt/C; total metal loading for anode/cathode: 2 mg cm^{-2}; 1 M CH_3OH, 0.2 MPa O_2, 90 °C [52].

2.3. The microemulsion method

Microemulsion method is a new route for synthesizing Pt–Ru catalysts that has been developed in recent years [53–58]. In this method, the first step is the formation of Pt–Ru nanoparticles through a water-in-oil microemulsion reaction, followed by a reduction step. Here the microemulsion serves as a nanoscaled reactor in which the chemical reaction takes place. The microemulsion is a nanoscaled aqueous liquid droplet containing a noble metal precursor. The droplets are engulfed by surfactant molecules and uniformly dispersed in an immiscibly continuous organic phase. The reduction step can be carried out either by adding a reducing agent (e.g., N_2H_4, HCHO, and $NaBH_4$) into the microemulsion system, or by mixing it with another reducing agent-containing microemulsion system. As a result, the reduction reaction is confined to the inside of the nanoscaled microemulsion, and the formed metal particle sizes can be easily controlled by the magnitude of the microemulsion size. The surfactant molecules can function as protective agents to prevent the Pt–Ru nanoparticles from agglomeration. The removal of surfactant molecules can be easily carried out by heat-treating high-surface-area carbon supported nanoparticles. Pt–Ru/C catalysts prepared by this method were found to exhibit higher activity than those commercially available for methanol oxidation in both electrochemical half-cell containing sulphuric acid and methanol [54] and in a DMFC [56]. Table 3 summarizes the literature results for Pt–Ru nanoparticle catalysts synthesized by the microemulsion method, together with their characterization and activity evaluation.

The main advantage of the microemulsion method is its ease in controlling metallic composition and particle size within a narrow distribution by varying the synthetic conditions. Liu et al. [53] studied the formation conditions of microemulsion in a (H_2PtCl_6 + $RuCl_3$ + NaOH)–(NP_5 + NP_9)–cyclohexane system. A limited region in the phase diagram was identified to be suitable for microemulsion formation. The microemulsion-

Table 3
Summary of the reported Pt–Ru/C catalysts synthesized by different routes of the microemulsion method

Catalyst	Water phase/oil phase	Reducing agent/surfactant	Particle size (nm)	Activity	Measurement protocol	Reference
40% $Pt_{50}Ru_{50}$	H_2PtCl_6, $RuCl_3$/cyclohexane	HCHO/NP5 + NP9	4.3 ± 1.6	0.03 mA cm^{-2} at 200 mV (vs. SCE), 0.008 mg cm^{-2}	CV (vitreous carbon) 1 M H_2SO_4 + 2 M CH_3OH, RT	[53]
20% $Pt_{50}Ru_{50}$	H_2PtCl_6, $RuCl_3$/cyclohexane	$NaBH_4$/AOT	4.5–6.0	10 mA cm^{-2} at 200 mV (vs. SCE), 0.5 mg cm^{-2}	Polarization (graphite) 1 M H_2SO_4 + 2 M CH_3OH, RT	[54]
20% $Pt_{50}Ru_{50}$	H_2PtCl_6, $RuCl_3$/cyclohexane	N_2H_4/TritonX-100	2.5 ± 0.2	7 mA cm^{-2} at 200 mV (vs. Ag/AgCl), 0.4 mg cm^{-2}	CV (carbon paper) 1 M H_2SO_4 + 0.5 M CH_3OH, RT	[55]
(Non-C) $Pt_{50}Ru_{50}$	H_2PtCl_6, $RuCl_3$/heptane	$NaBH_4$/VRIJ®30	4 ± 1	1000 A mol^{-1} at 400 mV (vs. RHE)	CV (gold disc) 0.5 M H_2SO_4 + 0.1 M CH_3OH, RT	[56]
20% $Pt_{50}Ru_{50}$	H_2PtCl_6, $RuCl_3$/heptane	$NaBH_4$/AOT	3–6	50 mA cm^{-2} at 400 mV, 1 mg cm^{-2}	A single DMFC, 3.0 M CH_3OH, O_2, 90 °C	[57]
40% $Pt_{50}Ru_{50}$	H_2PtCl_6, $Ru(NO)(NO_3))_3$/isooctane	N_2H_4/Berol050	3.2–13.7	0.02 mA cm^{-2} at 400 mV (vs. RHE), 0.01 mg cm^{-2}	CV (glassy carbon) 0.5 M $HClO_4$ + 1 M CH_3OH, 25 °C	[58]

produced Pt–Ru/C catalyst, which has smaller particle sizes, show higher anodic peak current density (0.24 mA $cm^{-2}_{(metal)}$) towards methanol oxidation in CV measurement, compared with the catalyst produced by a conventional emulsion method (0.05 mA $cm^{-2}_{(metal)}$). Zhang and Chan [55] synthesized some Pt–Ru/C catalysts by a two-microemulsion route, in which the metal precursors and reducing agent formed two individual microemulsion systems. Their catalysts exhibited a very narrow size distribution (2.5 ± 0.2 nm) and were highly alloyed, as shown by HRTEM and the electron diffraction pattern in Fig. 4. The relationship between Pt–Ru nanoparticle size and the metal precursor concentration displays two levels of stable particle size in the plot. The low particle size level appears to be the nucleation limit, which is the minimum size required for a stable particle to exist. The upper particle size level appears to be limited by the size of the microemulsion or the mass transfer limitation on growth. Xiong and Manthiram [57] reported that the nanoparticle size depends on the ratio (W) of water to surfactant (i.e.,

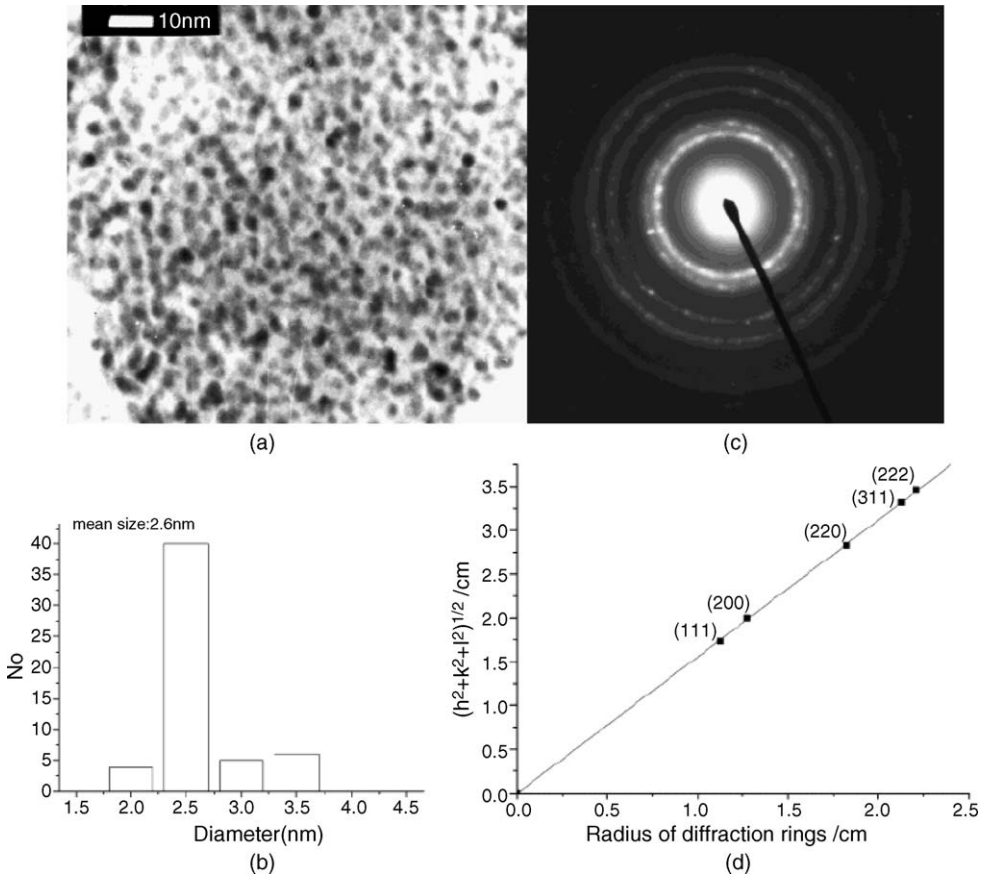

Fig. 4. (a) Transmission electron micrograph of Pt–Ru nanoparticles prepared by the microemulsion method. (b) Pt–Ru nanoparticle size distribution histogram. (c) Electron diffraction pattern of a region of the same sample. (d) Electron diffraction rings indexed in $h\,k\,l$ order [55].

sodium bis-(2-ethylhexyl)-sulfosuccinate (AOT)) in their case. They found that the Pt–Ru nanoparticle size increased initially with increasing W and became nearly constant when $W > 10$. These results demonstrated that a mono-size distribution could be easily obtained by controlling the synthetic conditions.

However, like the organometallic colloid method, the microemulsion method also uses costly surfactant molecules and requires a substantial number of separation and washing steps, which may be not suitable for large-scale production.

It is worthwhile to point out that the criteria for Pt–Ru catalyst evaluation in terms of composition, structure and particle size are still controversial. It is generally recognized that Pt–Ru catalysts with a Pt:Ru atomic ratio of 1:1 may be the best DMFC catalysts in terms of activity and stability [59]. However, Dubau et al. [60] reported recently that the best composition of Pt–Ru/C catalysts for methanol oxidation largely depends on electrode working potentials. A ruthenium-rich catalyst showed higher performance at lower potentials, while a platinum-rich catalyst was better at higher potentials. Contrary to the current understanding of Pt–Ru electrocatalyzed oxidation of methanol, Long et al. [61] argued that the Pt–Ru alloy is not the most desirable form of the catalyst. A mixed-phase Pt–RuO_xH_y catalyst showed better electrocatalytic activity than alloyed Pt–Ru catalyst. Other approaches, such as the deposition of Ru clusters onto Pt nanoparticles by Waszczuk et al. [62] and the deposition of Pt onto Ru nanoparticles by Sasaki et al. [63], can also form catalysts that show higher electrocatalytic activity compared with the commercially available alloyed Pt–Ru catalysts.

3. Catalyst supports

In order to achieve fine dispersion, high utilization and stable nanoscale metallic particles, catalyst-supporting strategies have been explored. Compared to bulk metal catalysts, supported catalysts show higher activity and stability. Carbon particles are frequently used as catalyst supports because of their relative stability in both acidic and basic media, good electric conductivity and high specific surface area. In the past, several carbon materials have been tested as catalyst supports for DMFCs. Carbon material has a strong influence on the properties of supported noble metal catalysts, such as metal particle size, morphology, size distribution, alloyed degree, stability and dispersion. On the other hand, carbon supports can also affect the performance of supported catalysts in fuel cells, such as mass transport and catalyst layer electronic conductivity, electrochemical active area, and metal nanoparticle stability during the operation. Hence, the optimization of carbon supports is very important in DMFC development. The properties of a suitable carbon support, such as specific surface area, porosity, morphology, surface functional groups, electronic conductivity, corrosion resistance, etc, must be down-selected in order to make an active catalyst. The properties of the carbon support materials have strong effects on the preparation procedures and performance of synthesized supported catalysts. The physical and chemical origins of those effects are not fully understood yet, although considerable efforts have been made in the last decades to optimize the supporting strategies in terms of theoretical and experimental approaches, especially in the DMFC area. In recent years numerous studies have concentrated on understanding the effects of carbon supports and exploring new carbon supports [64–104].

3.1. Carbon black

Carbon blacks are commonly used as supports for DMFC anode catalysts. There are many types of carbon blacks, such as Acetylene Black, Vulcan XC-72, Ketjen Black, etc., and these are usually manufactured by pyrolyzing hydrocarbons such as natural gas or oil fractions taken from petroleum processing. These carbon blacks show different physical and chemical properties, such as specific surface area, porosity, electrical conductivity and surface functionality. Among these factors, specific surface area has a significant effect on the preparation and performance of supported catalysts [64,65]. Generally, highly dispersed, supported catalysts cannot be prepared from low-surface-area carbon blacks (e.g., Acetylene Black). High-surface-area carbon blacks (e.g., Ketjen Black) could support highly dispersed catalyst nanoparticles. However, Ketjen Black supported catalysts showed high Ohmic resistance and mass transport limitation during fuel cell operation [2]. Vulcan XC-72 with a surface area of $\sim 250\,m^2\,g^{-1}$ has been widely used as a catalyst support, especially in DMFC anode catalyst preparation. An accessible and sufficiently large surface for maximum catalyst dispersion has been argued to be a necessary but insufficient condition for obtaining optimized carbon supported catalysts. Other factors, such as pore size and distribution, and surface functional groups of carbon blacks, also affect the preparation and performance of carbon black supported catalysts [66–71]. For example, in a conventional impregnation process, a portion of the metal nanoparticles may be sunk into the micropores of Vulcan XC-72. This portion inside the micropores has less or no electrochemical activity due to the difficulty in reactant accessibility. This is the major reason why some catalysts prepared by the impregnation method have not shown high activity even when the metal loading is very high. By keeping Pt nanoparticle size larger than the micropore size, Anderson et al. [67] found that the saturated weight loading of Pt onto Vulcan carbon by the colloid method was 9–10 wt.% versus 10–40 wt.% by the impregnation method. Their results indicated that micropores, which are smaller than the Pt nanoparticle size, could effectively block the sinking of the metal nanoparticles.

The contact between the metal nanoparticles and Nafion micelles in the catalyst layer of MEA is also affected by carbon support particle pore size and distribution. As reported by Uchida et al. [66], the Nafion ionomer has rather large (>40 nm) micelles. Metal nanoparticles residing in carbon pores below 40 nm in diameter have no access to the Nafion ionomer and do not contribute to the electrochemical activity. The metal catalyst utilization is determined by an electrochemical accessible active area rather than carbon specific surface area. Recently, Rao et al. [70] investigated the effect of carbon porosity on the specific activity of the Pt–Ru/C catalyst for methanol oxidation. They found that a higher content of small pores (<20 nm) containing metal particles where the Nafion ionomer could not easily

enter, resulted in poor contact between the metal nanoparticles and Nafion micelles and there was, therefore, a lower level of methanol oxidation activity. For example, 20% PtRu supported on Sib-19P ($S_{BET} = 72\ m^2\ g^{-1}$) showed a mass specific activity of 180 mA $mg^{-1}_{(metal)}$ at 500 mV during a DMFC half-cell testing, which is almost six times higher than that for PtRu/Sib-619P ($S_{BET} = 415\ m^2\ g^{-1}$). More recently, Wang et al. [71] reported that Vulcan XC-72 supported Pt–Ru catalysts showed improved catalytic activity towards methanol oxidation after the catalyst was pre-treated by ozone. CV results showed that the anodic peak current of ozone-treated sample was 1.5 times of that of untreated sample in an Ar-saturated 0.5 M CH_3OH + 0.5 M H_2SO_4 solution. This improvement contributed to the increase in surface concentration of the active functional oxygen containing groups on the ozone-treated Vulcan XC-72. These results indicate that some innovative approaches should be explored for catalyst activity and performance improvement and optimization.

3.2. Nanostructured carbon

In recent decades, a series of new nanostructured carbon materials were explored as catalyst supports. The family of carbon nanotubes (CNTs) is the most well-known nanostructured carbon, which has shown very promising results in catalyst support for fuel cell applications due to their unique electrical and structural properties. The reported studies have shown that CNTs were superior to carbon blacks as catalyst supports for proton exchange membrane fuel cells (PEMFCs) [72,73]. A CNT supported Pt catalyst with 12 wt.% Pt loading could give a 10% higher fuel cell voltage, and twice the power density than that of carbon black supported with 29 wt.% Pt loading [74,75]. On the other hand, many studies have explored CNTs as supports for DMFC catalysts in recent years. Li et al. [76–78] reported that multi-wall carbon nanotube (MWNT) supported catalysts exhibited better performance in DMFCs compared to those supported by carbon black (XC-72) under identical conditions both in half-cell characterization and in a fuel cell performance test. Their results showed that the mass activity of Pt/MWNT catalyst at 0.7 V (versus DHE) in a single cell testing was 14.7 mA $mg^{-1}_{(Pt)}$, much better than Pt/XC-72 catalyst (2.2 mA $mg^{-1}_{(Pt)}$). Che et al. [79] found that the current density of methanol oxidation on a Pt/MWNT catalyzed membrane electrode was 20 times higher than that of a bulk Pt electrode. Rajesh et al. [80,81] investigated methanol oxidation catalyzed by various metal catalysts that could be supported on CNTs and commercially available Vulcan carbon. The activity and stability of these electrodes were ranked from highest to lowest as: Pt–WO_3/CNT > Pt–Ru/Vulcan > Pt/CNT > Pt/Vulcan > bulk Pt. Single-wall carbon nanotube (SWNT) supported Pt electrodes were also reported to exhibit higher catalytic activity both for methanol oxidation and oxygen reduction than that seen in an unsupported Pt electrode [82]. The authors studied the kinetics of a methanol oxidation reaction on a Pt/SWCNT electrode and found that the onset potential of methanol oxidation on this electrode was ~200 mV versus SCE which was 200 mV lower than that of the unsupported Pt electrode (400 mV versus SCE). The higher catalytic activity was thereby attributed to the larger surface area of carbon nanotube architecture and the lower overpotential for methanol oxidation. Therefore, CNTs appear to have promising potential as catalyst supports for DMFCs.

However, the CNT synthesis, metal loading and electrode preparation based on CNT supports still face some challenges, especially when applied to fuel cells. CNTs are usually synthesized by carbon-arc discharge, laser ablation of carbon, or chemical vapor deposition (typically on catalytic particles). These synthetic methods have their limitations in terms of large-scale production and cost-effectiveness. Their harsh synthetic conditions and low production yields are major disadvantages. Currently, SWCNTs are produced only on a very small scale and the process is extremely costly [83]. It is necessary to further develop industrial large-scale production of CNTs to meet the needs of all the possible applications, including the fuel cell industry.

Metal nanoparticle loading onto CNTs with high dispersion is not an easy task. Several methods have been developed to prepare highly dispersed metal/CNT catalysts, as summarized in Table 4. The conventional impregnation method was frequently used to deposit metal nanoparticles onto CNTs [76,79,84]. Using this method, Che et al. [79] were able to deposit Pt–Ru alloy particles with a very narrow particle size distribution onto the CNT. However, conventional impregnation techniques based on wet impregnation and chemical reduction of the metal precursors are time consuming and the produced catalysts are easily contaminated by some side-products. Alternatively, the electrodeposition method has been used to make CNT supported catalysts because of its high-purity and simplicity [73,75,82,85]. The disadvantage of this method is difficult to estimate the loading of the metallic catalyst due to the concurrent reduction of protons. It was also difficult to attain small nanoparticles by

Table 4
Representative metal-loading methods of nanostructured carbon supported catalysts for DMFCs

Metal/support	Pre-treatment	Metal-loading methods	Particle size (nm)	Reference
Pt–Ru/CNT membrane	None	Impregnation in H_2PtCl_6 + $RuCl_3$ solutions	1.6	[79]
Pt/MWCNT	HNO_3–H_2SO_4	Impregnation in H_2PtCl_6 ethylene glycol solutions	2–4	[76]
Pt/CNT array	HNO_3	Electrodeposit in H_2PtCl_6 + HCl solutions	30–40	[75]
Pt/SWCNT/OTE	TOAB	Electrodeposit in H_2PtCl_6 solutions	20	[82]
Pt/MWCNT	None	Supercritical fluid reaction in $Pt(acac)_2$ + methanol solutions	5–10	[86]
Pt/GCNF	HCl	Impregnation in $(NH_3)_2Pt(NO_2)_2$ + ethanol solutions	3–7	[91]
Pt–Ru/CNC	HNO_3	Impregnation in H_2PtCl_6 + $RuCl_3$ solutions	2.3	[94]
Pt/C_{60}/OTE	None	Electrodeposit in H_2PtCl_6 + $LiClO_4$ solutions	100–150	[96]

electrodeposition method, as shown in Table 1. More recently, Lin et al. [86] used a supercritical fluids (SCFs) method as a rapid, direct, and clean approach to prepare Pt/CNT catalyst for DMFCs. It was claimed that the supercritical fluid technology could result in products (and processes) that are cleaner, less expensive, and of higher quality than those produced using conventional technologies and solvents.

Additionally, it was found that the surface modification of CNTs before metal deposition was important for achieving optimal interaction between the support and the catalyst precursor [87,88]. Because the pristine surface of CNTs is inert, it is difficult to attach metal nanoparticles to the substrate surface. Through surface modification or pre-treatments, some anchoring sites were introduced onto the surface so the metal nanoparticles could easily attach onto the CNTs surface. The most widely used pre-treatment is refluxing CNTs in a nitric acid to create an acid site on the surface, which can act as a nucleation center for metal ions.

Another challenge of CNTs as a catalyst support for DMFCs is how to use them to fabricate high performance working electrodes. If the electrode was prepared by a conventional ink process, it was estimated that only 20–30% of the platinum catalyst was utilized because of the difficulty for reactants to access inner electrocatalytic sites [82]. Developing new electrode structures could make use of CNTs' advantages of structural, electronic and mechanical properties. Recently, Sun et al. [89,90] developed some techniques to grow CNTs on the fuel cell carbon paper fibers to produce a three-dimensional nanotube-based hierarchical structure (Fig. 5). Platinum or platinum alloys are expected to deposit directly onto these novel CNT-based catalyst supports, which seems to be a promising way to make low-cost electrodes for DMFCs by increasing noble metal utilization.

In addition to CNTs, other nanostructured carbons, such as carbon nanofibers, carbon nanocoils and fullerenes, were also explored as catalyst supports for DMFCs. Graphitic carbon nanofibers (GCNFs) have three structure types: platelet, ribbon, and herring-bone. Bessel et al. [91] investigated the methanol oxidation activities of these three types of GCNF supported Pt catalysts. They found that the catalysts containing 5 wt.% Pt supported on platelet and ribbon GCNFs exhibited comparable activities to that catalyzed by 25 wt.% Pt supported on Vulcan carbon, while a herring-bone GCNF supported Pt catalyst showed poorer electrochemical activity. Steigerwalt et al. [92,93] also prepared highly dispersed Pt–Ru/GCNF catalysts and investigated their performance as an anode catalyst for DMFCs. A 50% increase in performance was observed compared to an unsupported Pt–Ru colloid anode catalyst. Recently, carbon nanocoils (CNCs), a new nanostructured carbon support, was synthesized by a solid-phase synthetic method and used as DMFC catalyst supports [94,95]. The authors prepared Pt–Ru/CNC and Pt–Ru/Vulcan catalysts with 60 wt.% metal loading, and compared their performance to commercially available E-TEK Pt–Ru/C catalyst for DMFCs. They found that, under identical testing conditions, the current density at 0.6 V catalyzed by a CNC-supported catalyst was 4 and 20 times higher, and the maximum power density was 170% and 230% higher than that of Vulcan supported catalyst and the commercial catalyst, respectively (Fig. 6). The excellent performance was attributed to the low electric resistance and the unique pore characteristics of CNCs, which favour the diffusion of methanol and the removal of CO_2 gas. More recently, a fullerene (C_{60}) film electrode was also suggested as a catalyst support for methanol oxidation after electrodeposition of Pt on these fullerene nanoclusters [96].

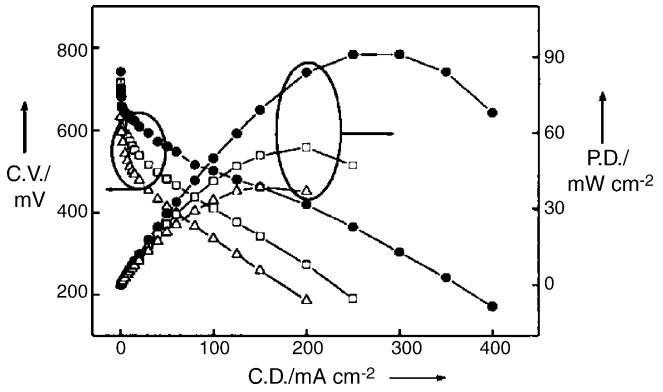

Fig. 6. Polarization curves for a DMFC using a Pt–Ru catalyst (60 wt.%) supported on carbon nanocoils (CNC, ●), Vulcan XC-72 (□) and a commercially available supported catalyst (△). CV, CD and PD stand for cell voltage, current density, and power density, respectively [94].

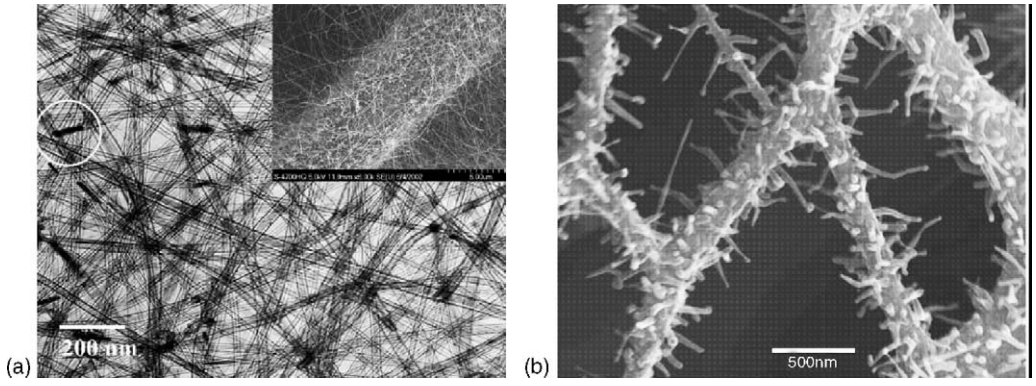

Fig. 5. (a) TEM micrograph of MWCNTs grown on the carbon fibers. Inset: SEM micrograph showing a high density of MWCNTs on the carbon fiber. (b) SEM micrograph of secondary MWCNTs grown on MWCNTs-on-carbon paper [89].

3.3. Mesoporous carbon

Mesoporous carbon used as catalyst support is another new area in DMFC anode catalysis [97]. Generally, a high performance DMFC anode requires an efficient three-phase reaction zone at nanoscale, in which the electrochemical reactions occur on the surface of the metal nanoparticle involving electron and proton transport. In addition, it also requires the provision of an efficient transport passage for liquid-phase reactants (CH_3OH, H_2O) and the gas-phase product (CO_2). Too many small micropores (<2 nm) in carbon supports (e.g., Vulcan XC 72) decreases catalyst utilization because the mass transport of reactants and product is poor in these micropores. When macroporous size is larger than 50 nm, the surface area will become small and the electrical resistance will increase [97]. Mesoporous carbons with tuneable pore sizes in the range 2–50 nm are, thus, attractive for use as catalyst supports and have the potential to enhance both the dispersion and utilization of metal catalysts.

The ordered mesoporous carbon is usually synthesized by a template method starting with either highly ordered mesoporous silica or nanosized silica spheres. With mesoporous silica or nanosized silica as a template, organic materials were diffused into the pores followed by carbonization. Uniform mesoporous carbon can be formed after removing the silica template by HF etching. Yu et al. [98,99] synthesized a series of porous carbons with pore sizes in the range 10–1000 nm by this procedure and investigated the performance of these porous carbon-supported Pt–Ru catalysts under DMFC conditions. They found that the porous carbon with a mesopore size (25 nm) showed the highest performance, which corresponds to a 43% increase in activity as compared to that of a commercially available Pt–Ru/C catalyst (E-TEK). This higher performance was considered to be not only due to the higher surface areas and larger pore volumes, which allowed a higher degree of catalyst dispersion, but also due to highly integrated interconnected pore systems with periodic order, which allowed efficient transport of reactants and products. Raghuveer and Manthiram [100,101] used a modified colloidal template route to control the pore size of porous carbon. The obtained mesoporous carbon produced larger surface area and pore volume than the Vulcan XC 72R (Table 5). They carried out the electrochemical measurements using catalyst-coated glassy carbon electrodes with a catalyst loading of 0.28 mg cm^{-2}, and found that the mesoporous carbon loaded with 5% Pt exhibited three times higher mass activity (mA mg^{-1} Pt) than the commercially available 20% Pt/C catalyst for methanol oxidation (Table 5). Recently, spherical carbon capsules with a hollow core and mesoporous shell structures (HCMS) were used to support the Pt–Ru catalyst [102]. The HCMS carbon supported catalysts exhibited higher specific activity towards methanol oxidation than the commonly used E-TEK catalyst by approximately 80%. In addition, the Mesocarbon microbead (MCMB), a type of spherical carbon particle with many nodular lumps and pores at its surface, was also investigated as Pt or Pt–Ru catalyst support for methanol oxidation [103,104]. Although the particle size of MCMB supported Pt–Ru nanoparticles is comparatively larger (12–13 nm), better performance compared to Vulcan XC 72R carbon support catalyst was observed. The overpotential of Pt–Ru/MCMB electrode was 0.39 V (versus SCE) at 300 mA cm^{-2}, which was 70 mV lower than that of Pt–Ru/Vulcan XC-72 electrode. Therefore, mesoporous carbons appear to have great potential for catalyst supports in DMFC anode catalysis because they can offer significant cost reduction by improving catalyst utilization and lowering the catalyst loading.

4. Combinatorial method for new catalyst activity down-selection

New catalyst activity down-selection by combinatorial methods is a new development in DMFC anode catalysis. To explore new catalysts in a fast way is one of the major objectives in DMFC R&D. Many studies have been involved for several decades in exploring Pt-based ternary and quaternary alloys, other noble metals, and even non-noble metal alloys and compounds as alternatives to the Pt–Ru anode catalyst, and some significant progress has been made. For example, tungsten and molybdenum oxides were demonstrated to be good surface promoters for improving Pt activity towards methanol oxidation due to their special "spillover" effect [2]. However, conventional catalyst exploring methods are labour intensive, time consuming and inefficient. A rapid and efficient screening approach is urgently needed to accelerate the discovery of new DMFC anode catalysts and catalyst activity optimization. The combinatorial method, which has been well developed in pharmaceutical industry and heterogeneous catalysis, thus, has become an

Table 5
Pore characteristics of mesoporous carbon and Vulcan XC 72R, and their activities towards methanol oxidation as Pt supports [100]

Carbon support	BET surface area (m^2 g^{-1})	Total pore volume (cm^3 g^{-1})	Micropore volume (cm^3 g^{-1})
Mesoporous carbon	890	1.05	0
Vulcan XC 72R	235	0.67	0.25

Electrocatalyst	Electrochemical active surface area of Pt (m^2 g^{-1})	Specific activity I_f (mA cm^{-2}) at +0.75 V vs. SCE	Mass activity I_f (mA mg^{-1} Pt) at +0.75 V vs. SCE
5% Pt/mesoporous carbon	212	62	215
5% Pt/Vulcan XC 72R	79	26	91
20% Pt/Vulcan XC 72R (Johnson Matthey)	133	83	73

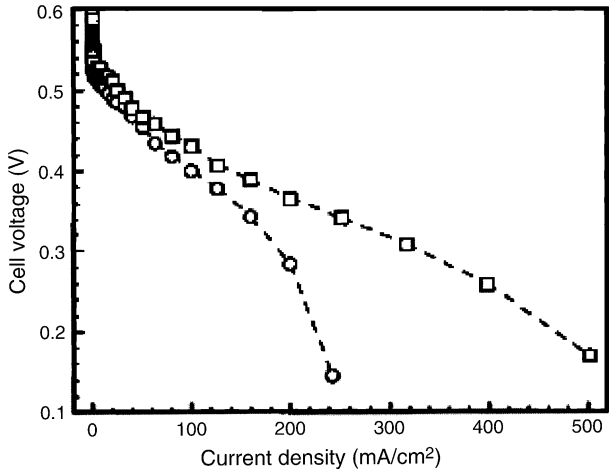

Fig. 7. Polarization curves of direct methanol fuel cells made from $Pt_{44}Ru_{41}Os_{10}Ir_5$ (□) and Johnson–Matthey $Pt_{50}Ru_{50}$ (◯) anode catalysts. Cathode: Pt; total metal loading for anode/cathode: 4.0 mg cm^{-2}; 0.5 M methanol, 10 psi air; 60 °C [108].

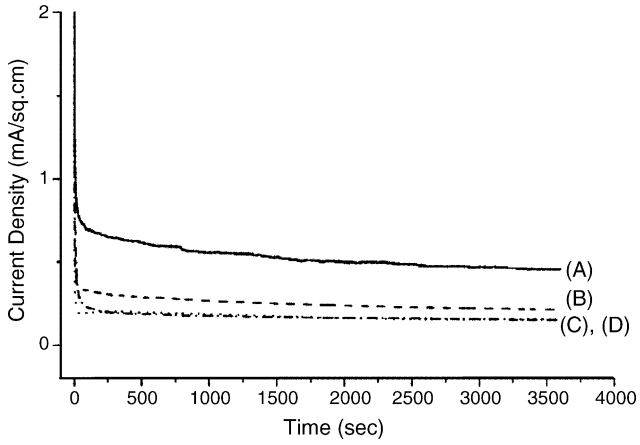

Fig. 8. Chronoamperometry curves of catalyst materials for methanol oxidation: (A) $Pt_{77}Ru_{17}Mo_4W_2$; (B) $Pt_{74}Ru_{20}Mo_4W_2$; (C) $Pt_{50}Ru_{50}$; and (D) $Pt_{82}Ru_{18}$. Potentiostatic oxidation of 2 M CH_3OH in 0.5 M H_2SO_4 deaerated with ultrahigh purity N_2 at 25 °C during the potential-step from 0.07 to 0.45 V (vs. RHE) [109].

appealing technique for discovering new catalysts for fuel cells, including DMFCs [105–107].

Reddington et al. [108] first reported a combinatorial method by using a fluorescence acid–base indicator to optically screen electrochemical catalysts for methanol oxidation. They prepared quaternary and five-pick-four arrays containing Pt, Ru, Os, Ir or Rh by inkjet printing and subsequent borohydride reduction. The indicator's fluorescence images, which respond to proton concentrations, were used to identify the activities of multi-component catalysts towards methanol oxidation. Using this combinatorial analysis, $Pt_{44}Ru_{41}Os_{10}Ir_5$ was deduced as the best quaternary formulation. A performance comparison of a $Pt_{44}Ru_{41}Os_{10}Ir_5$ catalyst prepared by borohydride reduction with a commercially available Pt–Ru catalyst showed that the former was significantly more active than the latter in DMFC testing at 60 °C (Fig. 7). Choi et al. [109] used a similar optical screening method to investigate quaternary catalysts containing W and Mo for methanol oxidation. They found that a quaternary catalyst with a formulation of $Pt_{77}Ru_{17}Mo_4W_2$ showed much better electrochemical activity and stability than $Pt_{50}Ru_{50}$ formulation (Fig. 8). In a 1 h potentiostatic oxidation, the steady-state current density of this quaternary catalyst on a glassy carbon electrode was nearly three times higher than that of $Pt_{50}Ru_{50}$ catalyst. After the potentiostatic oxidation, the following stationary anode polarization experiments also showed a voltage of 0.7 V (versus RHE) at 1.0 mA cm^{-2} for the quaternary catalyst, cf. 0.4 V (versus RHE) for $Pt_{50}Ru_{50}$ catalyst. As a simple and rapid approach, an optical screening method was also applied to optimize the Nafion-ionomer concentration in Pt–Ru catalysts with different compositions [110]. The authors found that the most active composition for methanol oxidation was $Pt_{50}Ru_{50}$/Nafion with a composition ratio of 63.6 wt.% Pt/36.4 wt.% Ru. However, the optical screening method, based on the proton concentration, has some disadvantages in identifying catalyst activity, especially when the electrolyte solution contains concentrated acid or base. The sensitivity is not high enough to distinguish minor activity differences between similar catalysts. It cannot provide direct electrochemical measurements that are finally required for complete characterization.

Electrochemical screening methods were then developed by several groups. Sullivan et al. [111] developed an automated electrochemical analysis system with a combinatorial 64-electrode array to measure proton concentration and electrochemical current at each electrode in a common electrolyte solution. They found that the direct electrochemical screening method has higher precision than an optical screening method in distinguishing small differences in current among differently modified electrodes. Guerin et al. [112] adopted a similar concept and constructed a cell consisting of a 64-element array containing vitreous carbon electrodes. Their system allowed a pseudo-parallel screening of catalysts deposited on independently addressable electrodes in a common electrolyte, using a single channel potentiostat and a multichannel current follower. They used this system to investigate CO electro-oxidation, oxygen reduction and methanol oxidation catalyzed by carbon-supported Pt catalysts with different metal loadings. Jiang and Chu [113] established another electrochemical screening system with a movable electrolyte probe containing both counter and reference electrodes that electrolytically contacted with the working electrode array and could be moved along the electrode array to address each electrode. This system, with fast response and good reproducibility, was used for down-selection of methanol oxidation catalysts in a variety of electrolyte solutions containing different reactant concentrations. Recently, Black et al. [114] explored the use of the scanning electrochemical microscope (SECM) as a characterization technique to combinatorially screen Pt–Ru catalyst activity. The results suggested that SECM could characterize electrocatalytic behaviour of fuel cell catalysts both qualitatively and quantitatively. However, this automated serial (from spot to spot) screening method may be relatively slower than parallel screening methods. Additionally, Hillier et al. [115–117] also employed SECM and scanning differential electrochemical mass spectrometry (SDEMS) as in situ characterization techniques for the combinatorial method. The addition of these advanced characterization techniques into the

combinatorial method makes the tool more powerful for the fuel cell catalyst down-selection process. On the other hand, in order to create a measurement environment similar to the real catalyst reaction conditions, Liu and Smotkin [118] developed an array membrane electrode assembly for screening DMFC anode catalysts. This screening device contained a 25-electrode array with actual fuel cell design features. State-of-the-art MEA fabrication techniques were used to prepare array electrodes. Each array electrode could be combined with a common counter electrode to form a miniaturized fuel cell. The electrochemical measurements were carried out using graphite flow field sensor electrodes and a multielectrode potentiostat. The performance of their array fuel cell was demonstrated by testing a series of Pt–Ru catalysts for methanol oxidation.

In addition to the screening characterization techniques, array preparation techniques are equally important to the development of the combinatorial method. A discovery level catalyst array needs a single synthetic method across a broad compositional phase space. Traditional catalyst preparation methods have difficulty meeting this requirement, because preparing such a large number of samples is labour intensive and time consuming. The routes of inkjet printing and subsequently borohydride reduction, as described in Refs. [108,109], were able to prepare large catalyst arrays with a broad composition distribution. Even so, it is difficult to prepare a homogeneous phase in a dot of the combinatorial array by this route. It is also difficult for borohydride reduction to produce high surface area catalysts, which may compromise the sensitivity of this method. For example, the PtRuOsIr catalyst showed superior performance compared with PtRu under the same preparation method of using borohydride reduction. However, the PtRu catalyst showed better performance when other state-of-the-art preparation methods were used [105].

Recently, other array preparation methods were reported by Whitacre et al. [119]. A combinatorial co-sputtering approach to screen fuel cell catalysts for methanol oxidation was carried out. Room-temperature sputter deposition was used to batch-fabricate multiple thin-film samples on a microfabricated Au multielectrode, which served as the current collector. A binary Pt–Ru system and a quaternary Ni–Zr–Pt–Ru system were examined by this combinatorial technique. X-ray diffraction (XRD), energy dispersive X-ray (EDX), and X-ray photoemission spectroscopy (XPS) results demonstrated that the sputter deposition method could create a smooth and fully homogeneous catalyst thin-film array, allowing the minimization of the morphology and segregation effects. Meanwhile, a low-Pt-content catalyst formulation of $Ni_{31}Zr_{13}Pt_{33}Ru_{23}$ was found to exhibit comparable specific activity of methanol oxidation to the best Pt–Ru alloy film in their studies (Fig. 9). This low-Pt-content catalyst showed a mass specific activity of 0.65 mA cm^{-2} mol_{Pt}^{-1} at 0.45 V (versus NHE) and 45 °C, cf. 0.38 mA cm^{-2} mol_{Pt}^{-1} for $Pt_{84}Ru_{16}$ catalyst. The results suggested that the catalytic process of $Ni_{31}Zr_{13}Pt_{33}Ru_{23}$ alloy, which could utilize Pt surface sites more efficiently, might be inherently different from that of the Pt–Ru alloys. Jayaraman et al. [120] reported an automated combinatorial screening system using pulsed potential electrodeposition to prepare catalyst arrays. This system was

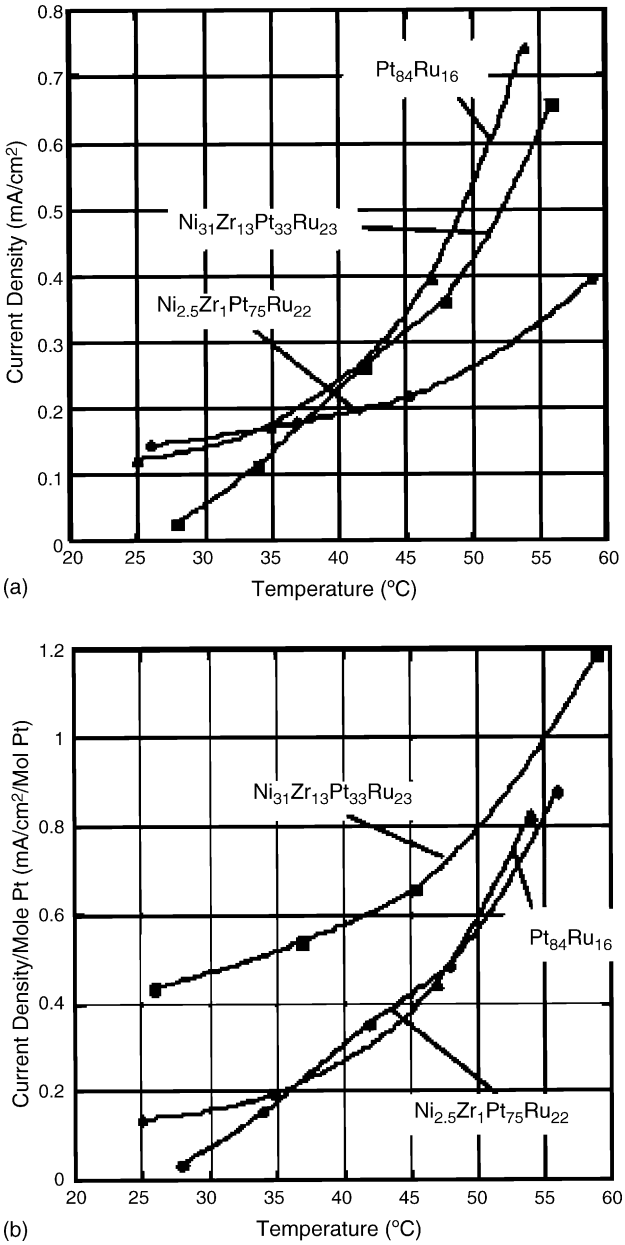

Fig. 9. (a) Specific activities (mA cm^{-2}) and (b) specific activities normalized to a Pt mole fraction (mA cm^{-2} mol^{-1} Pt) of $Ni_{31}Zr_{13}Pt_{33}Ru_{23}$, $Ni_{25}Zr_1Pt_{75}Ru_{22}$ and $Pt_{84}Ru_{16}$ alloy catalyst films as a function of temperature for methanol oxidation. The data of current densities were collected at 0.45 V (vs. NHE) after 300 s during steady-state potentiostatic experiments [119].

used to synthesize and screen Pt–WO_3 catalysts for methanol oxidation. XPS measurements revealed that the electrodeposited film is amorphous and not alloyed between Pt and W. The electrodeposition method has some limitations, especially in controlling the composition due to the different metal deposition rates. Alternatively, Jayaraman and Hillier [121,122] proposed multi-component gradient libraries to replace array libraries for combinatorial catalyst discovery. The gradient libraries showed a more complete and highly dense composition distribution than the array libraries. A novel 'gel-transfer' deposition procedure was used to synthesize the gradient libraries. This procedure included the localized diffusion of aqueous precursor metal salts

into a hydrated gel to establish spatially varying concentration fields, and then the electrodeposition of metals onto the substrate surface. This simple preparation method combined with mature screening methods seems very promising for a unique and powerful tool for the discovery of fuel cell catalysts.

5. Conclusions

Great progress has been made in developing preparation methods, carbon supports and down-selection approaches for DMFC anode catalysts in recent years. Several simple and tuneable methods (e.g., the glycol colloidal method and the spray pyrolysis method) have shown a superior ability to synthesize state-of-the-art Pt–Ru/C catalysts. Some new carbon materials, such as nano- and meso-structured carbons, have been demonstrated to be feasible as catalyst supports, although their applications still face some challenges in terms of synthesis, metal loading and electrode preparation. Combination of these advanced metal loading methods and excellent carbon supports could bring about a breakthrough in the exploration for a new generation of DMFC anode catalysts in the near future. The combinatorial method has shown great potential for fast catalyst down-selection, although the array preparation methods need to be further improved to reach realistic catalyst preparation conditions. Several catalyst formulations (e.g., $Ni_{31}Zr_{13}Pt_{33}Ru_{23}$) with low noble metal content and non-noble metal elements have been down-selected, and promising activity was claimed when compared to the current best Pt–Ru catalyst. Further development and improvement of this technology with respect to reliability, sensitivity, and repeatability will help the catalyst exploration process towards fuel cell commercialization.

Owing to the development of anode catalysts, the corresponding investigations of direct methanol single fuel cells have also achieved interesting performance. Current densities of 100–300 mA cm^{-2} at a cell potential of 400 mV have been reported for single cells operating at 60–90 °C, under pressurized air or oxygen, in 1.0–3.0 M methanol, and with metal loadings of 1.0–2.5 mg cm^{-2}. It is expected that the current density at 400 mV could reach 500 mA cm^{-2} after increasing the cell temperature to over 100 °C and optimizing the operation conditions. However, the performance of a direct methanol single fuel cell with a low-loading anode catalyst (<1.0 mg cm^{-2}) is still inferior to these values. The current results indicate that anode catalyst exploration including performance improvement and cost reduction remains a major challenge for DMFC R&D and therefore for commercialization in the future.

Acknowledgement

The authors would like to thank the Institute for Fuel Cell Innovation, National Research Council of Canada (NRC-IFCI) for financial support.

References

[1] S. Wasmus, A. Kuver, J. Electroanal. Chem. 461 (1999) 14–31.
[2] A.S. Arico, S. Srinivasan, V. Antonucci, Fuel Cells 2 (2001) 133–161.
[3] R. Dillon, S. Srinivasan, A.S. Arico, V. Antonucci, J. Power Sources 127 (2004) 112–126.
[4] A.K. Shukla, R.K. Raman, Annu. Rev. Mater. Res. 33 (2003) 155–168.
[5] C. Lamy, J.M. Leger, S. Srinivasan, in: J.O'M. Bockris, B.E. Conway, R.E. White (Eds.), Modern Aspects of Electrochemistry, vol. 34, 2001, pp. 53–118.
[6] M. Watanabe, S. Motoo, J. Electroanal. Chem. 60 (1975) 267–273.
[7] J.A.R. Van Veen, T. Frelink, W. Visscher, Surf. Sci. 335 (1995) 353–360.
[8] L. Zhang, J.J. Zhang, D.P. Wilkinson, H.J. Wang, J. Power Sources, doi:10.1016/j.jpowsour.2005.05.069.
[9] K.C. Lee, J.J. Zhang, H.J. Wang, D.P. Wilkinson, J. Appl. Electrochem., in press.
[10] C.K. Witham, W. Chun, T.I. Valdez, S.R. Narayanan, Electrochem. Solid-State Lett. 11 (2000) 497–500.
[11] W.C. Choi, S.I. Woo, J. Power Sources 124 (2003) 420–425.
[12] J. Chen, Z. Tao, S. Li, J. Am. Chem. Soc. 126 (2004) 3060–3061.
[13] Y. Takasu, T. Fujiwara, Y. Murakami, K. Sasaki, M. Oguri, T. Asaki, W. Sugimoto, J. Electrochem. Soc. 147 (2000) 4421–4427.
[14] E.S. Steigerwalt, G.A. Deluga, D.E. Cliffel, C.M. Lukehart, J. Phys. Chem. B 105 (2001) 8097–8101.
[15] H. William, A. Valdecir, R. Gonzalez, Electrochim. Acta 47 (2002) 3715–3722.
[16] E.S. Steigerwalt, G.A. Deluga, C.M. Lukehart, J. Phys. Chem. B 106 (2002) 760–766.
[17] N. Fujiwara, K. Yasuda, T. Ioroi, Z. Siroma, Y. Miyazaki, Electrochim. Acta 47 (2002) 4079–4084.
[18] N. Fujiwara, Y. Shiozaki, T. Tanimitsu, K. Yasuda, Y. Miyazaki, Electrochemistry 70 (2002) 988–993.
[19] C.W. Hills, N.H. Mack, R.G. Nuzzo, J. Phys. Chem. B 107 (2003) 2626–2636.
[20] A.J. Dickinson, L.P.L. Carrette, J.A. Collins, K.A. Friedrich, U. Stimming, Electrochim. Acta 47 (2002) 3733–3739.
[21] M. Neergat, D. Leveratto, U. Stimming, Fuel Cells 2 (2002) 25–30.
[22] K.A. Friedrich, L.P. Geyzers, A.J. Dickinson, U. Stimming, J. Electroanal. Chem. 524/525 (2003) 261–272.
[23] H. Qiao, M. Kunimatsu, N. Fujiwara, T. Okada, Electrochem. Solid-State Lett. 8 (2005) A175–A178.
[24] Y. Takasu, T. Kawaguchi, W. Sugimoto, Y. Murakami, Electrochim. Acta 48 (2003) 3861–3868.
[25] T. Kawaguchi, W. Sugimoto, Y. Murakami, Y. Takasu, Electrochem. Commun. 6 (2004) 480–483.
[26] Y. Zhang, A.M. Valiente, I.R. Ramos, Q. Xin, A.G. Ruiz, Catal. Today 93–95 (2004) 619–626.
[27] T. Kawaguchi, W. Sugimoto, Y. Murakami, Y. Takasu, J. Catal. 229 (2005) 176–184.
[28] M.S. Nashner, A.I. Frenkel, D. Somerville, C.W. Hills, J.R. Shapley, R.G. Nuzzo, J. Am. Chem. Soc. 120 (1998) 8093–8101.
[29] M.S. Nashner, A.I. Frenkel, D.L. Adler, J.R. Shapley, R.G. Nuzzo, J. Am. Chem. Soc. 119 (1997) 7760–7771.
[30] D.L. Boxall, G.A. Deluga, E.A. Kenik, W.D. King, C.M. Lukehart, Chem. Mater. 13 (2001) 891–900.
[31] W.D. King, J.D. Corn, O.J. Murphy, D.L. Boxall, E.A. Kenik, K.C. Kwiatkowski, S.R. Stock, C.M. Lukehart, J. Phys. Chem. B 107 (2003) 5467–5474.
[32] J.T. Moore, J.D. Corn, D. Chu, R. Jiang, D.L. Boxall, E.A. Kenik, C.M. Lukehart, Chem. Mater. 15 (2003) 3320–3325.
[33] T.C. Deivaraj, J.Y. Lee, J. Power Sources 142 (2005) 43–49.
[34] D.L. Boxall, G.A. Deluga, E.A. Kenik, W.D. King, C.M. Lukehart, Chem. Mater. 13 (2001) 891–900.
[35] B. Yang, Q. Lu, Y. Wang, L. Zhang, J. Lu, P. Liu, Chem. Mater. 15 (2003) 3552–3557.
[36] J.W. Guo, T.S. Zhao, J. Prabhuram, R. Chen, C.W. Wong, Electrochim. Acta 51 (2005) 754–763.
[37] M. Watanabe, M. Uchida, S. Motoo, J. Electroanal. Chem. 229 (1987) 395–406.
[38] V. Radmilovic, H.A. Gasteiger, P.N. Ross Jr., J. Catal. 154 (1995) 98–106.

[39] A.M.C. Luna, G.A. Camara, V.A. Paganin, E.A. Ticianelli, E.R. Gonzalez, Electrochem. Commun. 2 (2000) 222–225.
[40] H. Bönnemann, K.S. Nagabhushana, J. New. Mater. Electrochem. Syst. 7 (2004) 93–108.
[41] H. Bönnemann, W. Brijoux, R. Brinkmann, E. Dinjus, T. Joussen, B. Korall, Angew. Chem. 103 (1991) 1344–1346.
[42] T.J. Schmidt, M. Noeske, H.A. Gasteiger, R.J. Behm, P. Britz, W. Brijoux, H. Bönnemann, Langmuir 13 (1997) 2591–2595.
[43] T.J. Schmidt, M. Noeske, H.A. Gasteiger, R.J. Behm, P. Britz, W. Brijoux, H. Bönnemann, J. Electrochem. Soc. 145 (1998) 925–931.
[44] T.J. Schmidt, H.A. Gasteiger, R.J. Behm, Electrochem. Commun. 1 (1999) 1–49.
[45] U.A. Paulus, U. Endruschat, G.J. Feldmeyer, T.J. Schmidt, H. Bönnemann, R.J. Behm, J. Catal. 195 (2000) 383–393.
[46] H. Bönnemann, R. Brinkmann, S. Kinge, T.O. Ely, M. Armand, Fuel Cells 4 (2004) 289–296.
[47] M.T. Reetz, M.G. Koch, J. Am. Chem. Soc. 121 (1999) 7933–7934.
[48] X. Wang, I. Hsing, Electrochem. Acta 47 (2002) 2897–2981.
[49] T. Kim, M. Takahashi, M. Nagai, K. Kobayashi, Electrochem. Acta 50 (2004) 813–817.
[50] F. Bensebaa, N. Patrito, Y.L. Page, P.L. Ecuyer, D. Wang, J. Mater. Chem. 14 (2004) 3378–3384.
[51] Z. Liu, X. Ling, J. Lee, X. Su, L.M. Gan, J. Mater. Chem. 13 (2003) 3049–3052.
[52] X. Xue, T. Lu, C. Liu, W. Xing, Chem. Commun. 12 (2005) 1601–1603.
[53] Z. Liu, J.Y. Lee, M. Han, W. Chen, L.M. Gan, J. Mater. Chem. 12 (2002) 2453–2458.
[54] Y. Liu, X. Qiu, Z. Chen, W. Zhu, Electrochem. Commun. 4 (2002) 550–553.
[55] X. Zhang, K. Chan, Chem. Mater. 15 (2003) 451–459.
[56] J. Solla-Gullon, F.J. Vidal-Iglesias, V. Montiel, A. Aldaz, Electrochim. Acta 49 (2004) 5079–5088.
[57] L. Xiong, A. Manthiram, Solid State Ionics 176 (2005) 385–392.
[58] S. Rojas, F.J. Garcia, S. Jaras, M.V. Huerta, J.L.F. Fierro, M. Boutonnet, Appl. Catal. A: Gen. 285 (2005) 24–35.
[59] H.N. Dinh, X. Ren, F.H. Garzon, P. Zelenay, S. Gottesfeld, J. Electroanal. Chem. 491 (2000) 222–233.
[60] L. Dubau, C. Coutanceau, E. Garnier, J. Leger, C. Lamy, J. Appl. Electrochem. 33 (2003) 419–429.
[61] J.W. Long, R.M. Stroud, K.E. Swider-Lyons, D.R. Rolison, J. Phys. Chem. B 104 (2000) 9772–9776.
[62] P. Waszczuk, J. Solla-Gullon, H.S. Kim, Y.Y. Tong, V. Montiel, A. Aldaz, A. Wieckowski, J. Catal. 203 (2001) 1–6.
[63] K. Sasaki, J.X. Wang, M. Balasubramanian, J. McBreen, F. Uribe, R.R. Adzic, Electrochim. Acta 49 (2004) 3873–3877.
[64] A.S. Arico, S. Srinivasan, V. Antonucci, Fuel Cells 2 (2001) 133–161.
[65] Y. Takasu, T. Kawaguchi, W. Sugimoto, Y. Murakami, Electrochim. Acta 48 (2003) 3861–3868.
[66] M. Uchida, Y. Fukuoka, Y. Sugawara, H. Ohara, A. Ohta, J. Electrochem. Soc. 145 (1998) 3708–3713.
[67] M.L. Anderson, R.M. Stroud, D.R. Rolison, Nano Lett. 2 (2002) 235–240.
[68] G. Park, T. Yang, Y. Yoon, W. Lee, C. Kim, Int. J. Hydrogen Energy 28 (2003) 645–650.
[69] M. Mastragostino, A. Mossiroli, F. Soavi, J. Electrochem. Soc. 151 (2004) 1919–1924.
[70] V. Rao, P.A. Simonov, E.R. Savinova, G.V. Plaksin, S. Cherepanova, G. Kryukova, U. Stimming, J. Power Sources 145 (2005) 178–187.
[71] Z. Wang, G. Yin, P. Shi, Carbon 44 (2005) 133–140.
[72] Z. Liu, X. Lin, J.Y. Lee, W.S. Zhang, M. Han, L.M. Gan, Langmuir 18 (2002) 4054–4060.
[73] C. Wang, M. Waje, X. Wang, J.M. Tang, R.C. Haddon, Y. Yan, Nano Lett. 4 (2004) 345–348.
[74] T. Matsumoto, T. Komatsu, K. Arai, T. Yamazaki, M. Kijima, H. Shimizu, Y. Takasawa, J. Nakamura, Chem. Commun. (2004) 840–841.
[75] H. Tang, J.H. Chen, Z.P. Huang, D.Z. Wang, Z.F. Ren, L.H. Nie, Y.F. Kuang, S.Z. Yao, Carbon 42 (2004) 191–197.
[76] W. Li, C. Liang, J. Qiu, W. Zhou, H. Han, Z. Wei, G. Sun, Q. Xin, Carbon 40 (2002) 791–794.
[77] W. Li, C. Liang, J. Qiu, W. Zhou, A. Zhou, Z. Wei, G. Sun, Q. Xin, J. Phys. Chem. B 107 (2003) 6292–6299.
[78] W. Li, C. Liang, W. Zhou, J. Qiu, H. Li, G. Sun, Q. Xin, Carbon 42 (2004) 436–439.
[79] G. Che, B.B. Lakshmi, C.R. Martin, E.R. Fisher, Langmuir 15 (1999) 750–758.
[80] B. Rajesh, V. Karthik, S. Karthikeyan, K.R. Thampi, J.M. Bonard, B. Viswanathan, Fuel 81 (2002) 2177–2190.
[81] B. Rajesh, K.R. Thampi, J.M. Bonard, N.X. Xanthopoulos, H.J. Mathieu, B. Viswanathan, J. Phys. Chem. B 107 (2003) 2701–2708.
[82] G. Girishkumar, K. Vinodgopal, P. Kamat, J. Phys. Chem. B 108 (2004) 19960–19966.
[83] R.H. Baughman, A.A. Zakhidov, W.A. de Heer, Science 297 (2002) 787–792.
[84] Z. Liu, J.Y. Lee, W. Chen, M. Han, L.M. Gan, Langmuir 20 (2004) 181–187.
[85] Z. He, J. Chen, D. Liu, H. Tang, W. Deng, Y. Kuang, Mater. Chem. Phys. 85 (2004) 396–401.
[86] Y. Lin, X. Cui, C. Yen, C.M. Wai, J. Phys. Chem. B 109 (2004) 14410–14415.
[87] P. Serp, M. Corrias, P. Kalck, Appl. Catal. A 253 (2003) 337–358.
[88] H.I. Han, J.S. Lee, S.O. Park, S.W. Lee, Y.W. Park, H. Kim, Electrochim. Acta 50 (2004) 791–795.
[89] X. Sun, R. Li, B. Stansfield, J.P. Dodelet, S. Desilets, Chem. Phys. Lett. 394 (2004) 266–270.
[90] X. Sun, R. Li, B. Stansfield, J.P. Dodelet, S. Desilets, Int. J. Nanosci. 1 (2002) 223–234.
[91] C.A. Bessel, K. Laubernds, N.M. Rodriguez, R.T.K. Baker, J. Phys. Chem. 105 (2001) 1115–1118.
[92] E.S. Steigerwalt, G.A. Deluga, D.E. Cliffel, C.M. Lukehart, J. Phys. Chem. 105 (2001) 8097–8101.
[93] E.S. Steigerwalt, G.A. Deluga, C.M. Lukehart, J. Phys. Chem. 106 (2002) 760–766.
[94] T. Heon, S. Han, Y. Sung, K. Park, Y. Kim, Angew. Chem. Int. Ed. 42 (2003) 4352–4356.
[95] K. Park, Y. Sung, S. Han, Y. Yun, T. Hyeon, J. Phys. Chem. 108 (2004) 939–944.
[96] K. Vinodgopal, M. Haria, D. Meisel, P. Kamat, Nano Lett. 4 (2004) 415–418.
[97] K.Y. Chan, J. Ding, J. Ren, S. Cheng, K.Y. Tsang, J. Mater. Chem. 14 (2004) 505–516.
[98] J.S. Yu, S. Kang, S.B. Yoon, G. Chai, J. Am. Chem. Soc. 124 (2002) 9382–9383.
[99] G.S. Chai, S.B. Yoon, J.S. Yu, J.H. Choi, Y.E. Sung, J. Phys. Chem. B 108 (2004) 7074–7079.
[100] V. Raghuveer, A. Manthiram, Electrochem. Solid-State Lett. 7 (2004) 336–339.
[101] V. Raghuveer, A. Manthiram, J. Electrochem. Soc. 152 (2005) 1504–1510.
[102] G.S. Chai, S.B. Yoon, J.H. Kim, J.S. Yu, Chem. Commun. (2004) 2766–2767.
[103] Y.C. Liu, X.P. Qiu, Y.Q. Huang, W.T. Zhu, J. Power Sources 111 (2002) 160–164.
[104] Y.C. Liu, X.P. Qiu, Y.Q. Huang, W.T. Zhu, Carbon 40 (2002) 2375–2380.
[105] E.S. Smotkin, R.R. Diaz-Morales, Annu. Rev. Mater. Res. 33 (2003) 557–579.
[106] V.C. Choi, M.K. Jeon, Y.J. Kim, S.I. Woo, W.H. Hong, Catal. Today 93–95 (2004) 517–522.
[107] S.I. Woo, Y.J. Kim, H.Y. Cho, K.S. Oh, M.K. Jeon, N.H. Tarte, T.S. Kim, A. Mahmood, QSAR Comb. Sci. 24 (2004) 138–154.
[108] E. Reddington, A. Sapienza, B. Gurau, R. Viswanathan, S. Sarangapani, E.S. Smotkin, T.E. Mallouk, Science 280 (1998) 1735–1737.
[109] W.C. Choi, J.D. Kim, S.I. Woo, Catal. Today 74 (2002) 235–240.
[110] Y.-H. Chu, Y.G. Shul, W.C. Choi, S.I. Woo, H.-S. Han, J. Power Sources 118 (2003) 334–341.

[111] M.G. Sullivan, H. Utomo, P.J. Fagan, M.D. Ward, Anal. Chem. 71 (1999) 4369–4375.
[112] S. Guerin, B.E. Hayden, C.E. Lee, C. Mormiche, J.R. Owen, A.E. Russell, B. Theobald, D. Thompsett, J. Comb. Chem. 6 (2004) 149–158.
[113] R. Jiang, D. Chu, J. Electroanal. Chem. 527 (2002) 137–142.
[114] M. Black, J. Cooper, P. McGinn, Meas. Sci. Technol. 16 (2005) 174–182.
[115] B.C. Shah, A.C. Hillier, J. Electrochem. Soc. 147 (2000) 3043–3048.
[116] K. Jambunathan, A.C. Hillier, J. Electrochem. Soc. 150 (2003) 312–320.
[117] K. Jambunathan, S. Jayaraman, A.C. Hillier, Langmuir 20 (2004) 1856–1863.
[118] R. Liu, E.S. Smotkin, J. Electroanal. Chem. 535 (2002) 49–55.
[119] J.F. Whitacre, T. Valdez, S.R. Narayanan, J. Electrochem. Soc. 152 (2005) 1780–1789.
[120] S. Jayaraman, S.H. Baeck, T.F. Jaramillo, A.K. Shwarsctein, E.W. McFarland, Rev. Sci. Instrum. 76 (2005) 062227.
[121] S. Jayaraman, A.C. Hillier, J. Comb. Chem. 6 (2004) 27–31.
[122] S. Jayaraman, A.C. Hillier, Meas. Sci. Technol. 16 (2005) 5–13.